

Dynamics of quantum coherence and quantum phase transitions in XY spin systems

Meng Qin,^{1,*} Zhongzhou Ren,^{2,3,†} and Xin Zhang²

¹*Department of General Education, Army Engineering University of PLA, Nanjing 211101, China*

²*Department of Physics and Key Laboratory of Modern Acoustics, Nanjing University, Nanjing 210093, China*

³*School of Physics Science and Engineering, Tongji University, Shanghai 200092, China*



(Received 17 December 2017; published 3 July 2018)

We provide an analysis on the critical property of quantum coherence in XY spin systems based on the quantum renormalization group theory. We find that the quantum coherence obeys a conservation relation, i.e., the quantum coherence of a three-block state that is the sum of its reduced state coherence. The quantum coherence of the whole block state and its reduced state obey similar scaling properties with identical quantum coherence exponent 0.999. This means that the quantum critical behavior of a system may gain from its reduced state. With the unitary operator approaches, we evaluated the evolutionary characteristics of the large-scale system and illustrate its behavior with different initial states. The result shows that quantum coherence periodically fluctuates over time. The period decreases under the system size increasing.

DOI: [10.1103/PhysRevA.98.012303](https://doi.org/10.1103/PhysRevA.98.012303)

I. INTRODUCTION

Two homochromous light waves are coherent if they have the same frequency and a constant phase relationship [1]. Such results also exist in quantum physics, e.g., the electrons can be used as resources in Young's double-slit experiment. The reasons why all particles have wavelike properties can be explained by quantum superposition principle. It says that if $|\psi_1\rangle, |\psi_2\rangle, \dots$ are distinct states of a quantum system, then any superposition $|\psi\rangle = c_1|\psi_1\rangle + c_2|\psi_2\rangle + \dots = \sum_i c_i|\psi_i\rangle$ should also be another valid quantum state of the system, where $\sum_i c_i^2 = 1$ [2,3]. On the one hand, the quantum superposition principle is directly related to measurement and the results are expressed by probability. On the other hand, it is the superposition of the wave function rather than the probability and that induces interference phenomena. So, quantum coherence comes from the quantum superposition principle. In recent years, it has become the core concept in quantum information processing similar to quantum correlation [4].

The investigation of coherence has a long history. From Young's double-slit experiment to quantum optics and then quantum information science all have had much study. Surely we could get quantum coherence information with the aid of quantum state tomography in the past. The matrix of the state can be got through such measure, and the dynamics of off-diagonal elements reflects the quantum coherence in the system. But the quantum state tomography procedure is complex and tedious [5,6], especially as the nondiagonal matrix component increases exponentially with an increase of the system dimension.

In 2014, Baumgratz *et al.* defined the quantum coherence from the perspective of quantum resource [7]. They gave two kinds of quantitative measures for the d -dimensional quantum

systems, l_1 norm coherence and relative entropy coherence. Meanwhile, Girolami presented another quantum coherence method using the Wigner-Yanase skew information and it can be effectively observed in experiment [8]. These pioneering work lays a theoretical foundation for researchers to quantify the quantum coherence in the physical system. A great deal of study [8] also was stimulated by their research [9–18]. For example, Wang *et al.* establish “a method to measure coherence directly using its most essential behavior—the interference fringes [5].” Ma *et al.* find how to convert quantum coherence to quantum correlations [18].

In this study, relating quantum phase transitions, we address interesting topics on how to use quantum coherence to reflect quantum critical behavior. Karpat *et al.* have found some meaningful result that the local quantum coherence can reveal the occurrence of the second-order phase transition in the XY model [19]. But the quantum coherence of a block state and the dynamics behavior of the model are not discussed. Especially the following questions still need to answer. Do the finite-size scaling behaviors of coherence exist in the model? Can we estimate the accurate correlation length exponent by quantum coherence? Based on quantum renormalization group theory, we present some results for the above questions by investigating the one-dimensional XY model. The nonanalytic behavior and scaling behavior are also examined. Furthermore, we show low energy-state dynamics described by the time unitary operator. We investigate the evolution of the system under different initial states and illustrate how quantum coherence varies as a function of time.

This paper is organized as follows. In the next section, we will give an introduction to the quantum coherence. In Sec. III, the one-dimensional XY systems and the analytical results of quantum coherence are given. In Sec. IV, the critical behavior, nonanalytic behavior, and scaling behavior are presented. In Sec. V, the evolution of this system under the quantum renormalization group is given. The last section is a summary of our work.

*qrainm@gmail.com

†zren@tongji.edu.cn

II. QUANTUM COHERENCE

Baumgratz *et al.* [7] proposed l_1 norm coherence in 2014. This quantity meets the general requirement that a valid measure of quantum coherence should be satisfied. For a quantum state ρ , the l_1 norm coherence measures quantum coherence in a direct way; it's defined by the off-diagonal elements of ρ [7],

$$\text{QC}_{l_1}(\rho) = \sum_{\substack{i,j \\ i \neq j}} |\rho_{i,j}|. \quad (1)$$

This measure is the basic definition in quantifying quantum coherence in any system. Not only should all the requirements of a good coherence measure be obeyed, but also it is very easy to compute.

III. MODEL DESCRIPTION AND QUANTUM RENORMALIZATION GROUP

The Hamiltonian of a one-dimensional XY model reads [20]

$$H = J/4 \sum_{i=1}^N [(1 + \gamma)\sigma_i^x \sigma_{i+1}^x + (1 - \gamma)\sigma_i^y \sigma_{i+1}^y], \quad (2)$$

where J is the exchange interaction, γ is the anisotropy parameter, and σ^τ ($\tau = x, y$) are standard Pauli operators at site i . To keep the symmetry of the system and use majority rule, we select three sites as one block. Such three-site blocks can be viewed as one site in renormalized subspace. A schematic diagram can be seen in Fig. 1.

After separating the whole systems, the Hamiltonian can be divided as the block Hamiltonian H^B and interacting Hamiltonian H^{BB} , respectively,

$$H^B = J/4 \sum_L^{N/3} [(1 + \gamma)(\sigma_{L,1}^x \sigma_{L,2}^x + \sigma_{L,2}^x \sigma_{L,3}^x) + (1 - \gamma)(\sigma_{L,1}^y \sigma_{L,2}^y + \sigma_{L,2}^y \sigma_{L,3}^y)], \quad (3)$$

$$H^{BB} = J/4 \sum_L^{N/3} [(1 + \gamma)\sigma_{L,3}^x \sigma_{L+1,1}^x + (1 - \gamma)\sigma_{L,3}^y \sigma_{L+1,1}^y]. \quad (4)$$

The eigenvalues and eigenstates of the corresponding L th block are

$$d_1 = d_2 = d_3 = d_4 = 0, \\ d_5 = d_6 = \frac{J\sqrt{2\gamma^2 + 2}}{2},$$

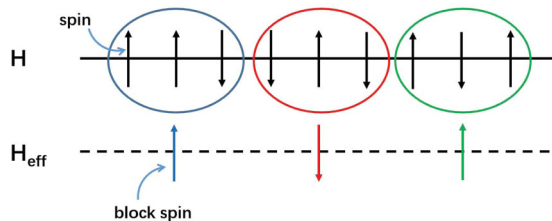


FIG. 1. A schematic description of QRG for three sites as one block.

$$d_7 = d_8 = -\frac{J\sqrt{2\gamma^2 + 2}}{2},$$

$$|\psi_1\rangle = \frac{1}{\sqrt{2}}(-|001\rangle + |100\rangle),$$

$$|\psi_2\rangle = \frac{1}{\sqrt{\gamma^2 + 1}}(-|000\rangle + \gamma|101\rangle),$$

$$|\psi_3\rangle = \frac{1}{\sqrt{2}}(-|011\rangle + |110\rangle),$$

$$|\psi_4\rangle = \frac{1}{\sqrt{\gamma^2 + 1}}(-\gamma|010\rangle + |111\rangle),$$

$$|\psi_5\rangle = \frac{1}{2\sqrt{1 + \gamma^2}}(\sqrt{1 + \gamma^2}|001\rangle + \sqrt{2}|010\rangle$$

$$+ \sqrt{1 + \gamma^2}|100\rangle + \sqrt{2}\gamma|111\rangle),$$

$$|\psi_6\rangle = \frac{1}{2\sqrt{1 + \gamma^2}}(\sqrt{1 + \gamma^2}|011\rangle + \sqrt{2}|101\rangle$$

$$+ \sqrt{1 + \gamma^2}|110\rangle + \sqrt{2}\gamma|000\rangle),$$

$$|\psi_7\rangle = \frac{1}{2\sqrt{1 + \gamma^2}}(-\sqrt{1 + \gamma^2}|001\rangle + \sqrt{2}|010\rangle$$

$$- \sqrt{1 + \gamma^2}|100\rangle + \sqrt{2}\gamma|111\rangle),$$

$$|\psi_8\rangle = \frac{1}{2\sqrt{1 + \gamma^2}}(\sqrt{1 + \gamma^2}|011\rangle - \sqrt{2}|101\rangle$$

$$+ \sqrt{1 + \gamma^2}|110\rangle - \sqrt{2}\gamma|000\rangle). \quad (5)$$

To get the critical properties of the system at absolute zero, we eliminate the excited state by integrals and only retain the ground-state parts. The projection operator is built for this aim. The relation between the original Hamiltonian and the effective Hamiltonian is associated by the projection operator, which is constructed by the two lowest eigenstates,

$$T = \prod_{i=1}^{N/3} T^L = \prod_{i=1}^{N/3} (|\uparrow\rangle_L \langle\psi| + |\downarrow\rangle_L \langle\psi|), \quad (6)$$

where $|\uparrow\rangle, |\downarrow\rangle$ are renamed states of each block to represent the effective site degrees of freedom. $|\psi\rangle$ is the ground state corresponding to the eigenvalue $-\frac{J\sqrt{2\gamma^2+2}}{2}$. The effective Hamiltonian is defined by

$$H_{\text{eff}} = T^\dagger H T = H_{\text{eff}}^0 + H_{\text{eff}}^1 = T^\dagger H^B T + T^\dagger H^{BB} T. \quad (7)$$

The form of effective Hamiltonian are similar to the original Hamiltonian,

$$H_{\text{eff}} = J'/4 \sum_L^{N/3} [(1 + \gamma')\sigma_L^x \sigma_{L+1}^x + (1 - \gamma')\sigma_L^y \sigma_{L+1}^y], \quad (8)$$

here the renormalized couplings are

$$J' = J \frac{3\gamma^2 + 1}{2 + 2\gamma^2}, \quad \gamma' = \frac{\gamma^3 + 3\gamma}{3\gamma^2 + 1}. \quad (9)$$

Following the renormalization equation, the nontrivial fixed point (critical point) γ_c can be gotten by solving $\gamma' = \gamma$. After some algebra, we can get the nontrivial fixed point $\gamma_c = 0$ and the trivial fixed point $\gamma = 1$. When $\gamma = 0$, the system is in

the spin-fluid phase. When $0 < \gamma \leq 1$, the system is in the Ising-like phase.

This enables us to compute the correlation length critical exponent ν defined as $\xi \sim |\gamma - \gamma_c|^{-\nu}$, i.e.,

$$\nu = \log_3 \left. \frac{d\gamma'}{d\gamma} \right|_{\gamma=\gamma_c}. \quad (10)$$

From the analytical solution at the thermodynamic limit, the critical points of the Heisenberg XY model are $\gamma_c = 0$. The correlation length critical exponents are $\nu = 1$ accordingly. The divergent critical property of the correlation length implies that the QRG measure can catch the long-distance critical behavior which is independent of the model details [21].

The ground-state density matrix is given by

$$\rho = \begin{pmatrix} 0 & 0 & 0 & 0 & 0 & 0 & 0 & 0 \\ 0 & \frac{1}{4} & -\frac{\sqrt{2}}{4k} & 0 & \frac{1}{4} & 0 & 0 & -\frac{\sqrt{2}\gamma}{4k} \\ 0 & -\frac{\sqrt{2}}{4k} & \frac{1}{2k^2} & 0 & -\frac{\sqrt{2}}{4k} & 0 & 0 & \frac{\gamma}{2k^2} \\ 0 & 0 & 0 & 0 & 0 & 0 & 0 & 0 \\ 0 & \frac{1}{4} & -\frac{\sqrt{2}}{4k} & 0 & \frac{1}{4} & 0 & 0 & -\frac{\sqrt{2}\gamma}{4k} \\ 0 & 0 & 0 & 0 & 0 & 0 & 0 & 0 \\ 0 & 0 & 0 & 0 & 0 & 0 & 0 & 0 \\ 0 & -\frac{\sqrt{2}\gamma}{4k} & \frac{\gamma}{2k^2} & 0 & -\frac{\sqrt{2}\gamma}{4k} & 0 & 0 & \frac{\gamma^2}{2k^2} \end{pmatrix}, \quad (11)$$

where $k = \sqrt{1 + \gamma^2}$.

According to the definition of quantum coherence, we can easily get the l_1 norm coherence of ρ ,

$$QC_{l_1}(\rho) = \sqrt{2}/k + 1/2 + (\sqrt{2}|\gamma|)/k + |\gamma|/k^2. \quad (12)$$

If we trace the first, second, or the third block spin separately, and then we derive the reduced density matrix,

$$\rho_{13} = \frac{1}{4(\gamma^2 + 1)} \begin{pmatrix} 2 & 0 & 0 & 2\gamma \\ 0 & \gamma^2 + 1 & \gamma^2 + 1 & 0 \\ 0 & \gamma^2 + 1 & \gamma^2 + 1 & 0 \\ 2\gamma & 0 & 0 & 2\gamma^2 \end{pmatrix}, \quad (13)$$

$$\rho_{12} = \frac{1}{4(\gamma^2 + 1)} \begin{pmatrix} \gamma^2 + 1 & 0 & 0 & -\gamma\sqrt{2\gamma^2 + 2} \\ 0 & \gamma^2 + 1 & -\sqrt{2\gamma^2 + 2} & 0 \\ 0 & -\sqrt{2\gamma^2 + 2} & 2 & 0 \\ -\gamma\sqrt{2\gamma^2 + 2} & 0 & 0 & 2\gamma^2 \end{pmatrix}, \quad (14)$$

$$\rho_{23} = \frac{1}{4(\gamma^2 + 1)} \begin{pmatrix} \gamma^2 + 1 & 0 & 0 & -\gamma\sqrt{2\gamma^2 + 2} \\ 0 & 2 & -\sqrt{2\gamma^2 + 2} & 0 \\ 0 & -\sqrt{2\gamma^2 + 2} & \gamma^2 + 1 & 0 \\ -\gamma\sqrt{2\gamma^2 + 2} & 0 & 0 & 2\gamma^2 \end{pmatrix}. \quad (15)$$

Following the l_1 norm coherence, we obtain the coherence of ρ_{13} , ρ_{12} , and ρ_{23} as

$$QC_{l_1}(\rho_{13}) = \frac{1}{2} + \frac{|\gamma|}{\gamma^2 + 1},$$

$$QC_{l_1}(\rho_{12}) = C_{l_1}(\rho_{23}) = \frac{\sqrt{2}}{2\sqrt{\gamma^2 + 1}} + \frac{\sqrt{2}|\gamma|}{2\sqrt{\gamma^2 + 1}}. \quad (16)$$

It is interesting to find that there exists a relation between Eq. (12) and Eq. (16),

$$QC_{l_1}(\rho) = QC_{l_1}(\rho_{13}) + QC_{l_1}(\rho_{12}) + QC_{l_1}(\rho_{23}). \quad (17)$$

IV. RENORMALIZED QUANTUM COHERENCE

A. The critical behavior of quantum coherence

In this section, we study the behavior of quantum coherence with the increase of system size. To give more intuitive results, we replace γ with g , i.e., $g = (1 + \gamma)/(1 - \gamma)$. Such a way can help us to deduce the result and to compare with Ref. [20]. We have plotted quantum coherence of ρ_{123} , ρ_{13} , and ρ_{12} versus g at different QRG steps in Fig. 2. As seen from Fig. 2, the plots of quantum coherence will become more pronounced at $g_c = 1$ ($\gamma = 0$) as the number of QRG increases. The $g_c = 1$ ($\gamma = 0$) is the critical point and the quantum coherence shows nonanalytic behavior in this point. In the thermodynamic limit, the QPT in the XY model separates

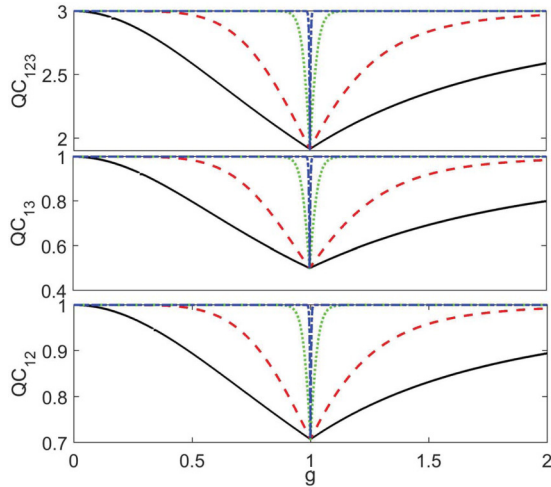


FIG. 2. Quantum coherence of ρ_{123} , ρ_{13} , and ρ_{12} as a function of g at different QRG iteration steps. Black solid line means 0th QRG step, red dashed line means 1st QRG step, green dotted line means 3rd QRG step, and blue dot-dashed line means 5th QRG step. The meaning of the term “step” is discussed in the appendix. All the parameters are dimensionless.

two different phases, the Ising-like phase where the quantum coherence is 3, 1, and 1, and the spin-fluid phase where the quantum coherence is 1.9142, 0.5, and 0.7071, respectively. As opposed to entanglement, for $0 \leq g < 1$ and $g > 1$ quantum coherence does not fall to 0 but approaches a stable value.

B. Nonanalytic behavior and scaling behavior

We have shown how to scale a large size system into a three-block state by the QRG procedure. Therefore, the coherence in the three-block state is the whole coherence in the finite-dimensional system. Every part contains the $N/3$ spin. Similar to entanglement and quantum correlation, the block coherence also can catch the critical point. From Refs. [20,22–25] we know that the correlation length will diverge at the critical point. The entanglement or quantum correlation shows scaling behavior at the critical point. This brings up the question of whether the quantum coherence will show the scaling property.

In Fig. 3, we plot the first derivative of the quantum coherence $|dQC/dg|_{\max}$ as a function of g . The derivative of three kinds of quantum coherence diverges as QRG increases, which indicates that the second-order QPT happened at this point. The scaling behavior can be found in the next figure.

The scaling behavior of the logarithm of $|dQC/dg|_{\max}$ versus the logarithm of system size $\ln(N)$ can be found in Fig. 4. The quantum coherences of ρ_{123} , ρ_{13} , and ρ_{12} all manifest scaling behavior near the quantum phase transition point. The finite-size scaling law is $|dQC/dg|_{\max} \sim N^{0.999}$. The critical exponents are associated with the correlation length exponent ν . At the critical point, the correlation length exponent ν reflects the behavior of correlation length ξ by $\xi \sim (g - g_c)^{-\nu}$. For the n th QRG iteration the correlation length changes to $\xi_n \sim (g_n - g_c)^{-\nu}$, which causes an expression $|\frac{dg_n}{dg}|_{g_c} \sim N^{1/\nu}$ in terms of ν and the number of sites in each block [21]. It is exactly the reciprocal of the correlation length exponent, i.e.,

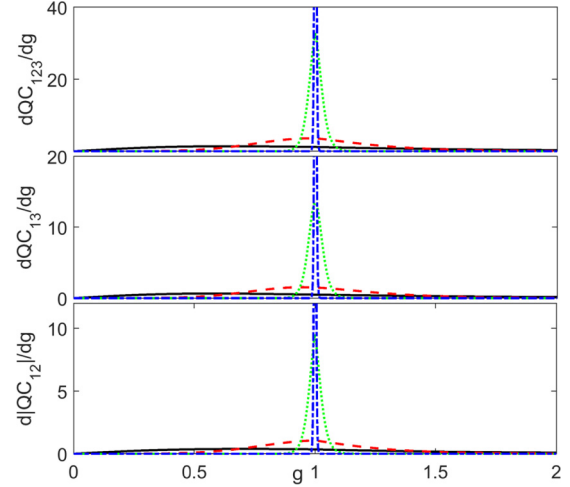


FIG. 3. The first derivative of the quantum coherence of ρ_{123} , ρ_{13} , and ρ_{12} as a function of g at different QRG iteration steps. Black solid line means 0th QRG step, red dashed line means 1st QRG step, green dotted line means 3rd QRG step, and blue dot-dashed line means 5th QRG step. All the parameters are dimensionless.

$\theta = 1/\nu$ [21]. Figure 4 displays $\theta \approx 0.999$, which is consistent with the exact result $\theta \approx 1$.

Apparently, the three critical exponents are identical. These results demonstrate that the critical exponent of ρ_{123} can be gotten through states ρ_{13} and ρ_{12} in the thermodynamic limit. On one hand, coarse graining in the renormalization group is beneficial to us; on the other hand, it can assist us in solving many complicated problems if such conservation relation exist. We may get the results of the whole system through investigating its reduced density matrix and then reduce the computational complexity and increase convenience.

V. EVOLUTION OF QUANTUM COHERENCE

Dynamics depicts how a quantum state evolves over time. From the above Hamiltonian, the eigenvalues and eigenstates of the model are derived and thus, the density matrix of

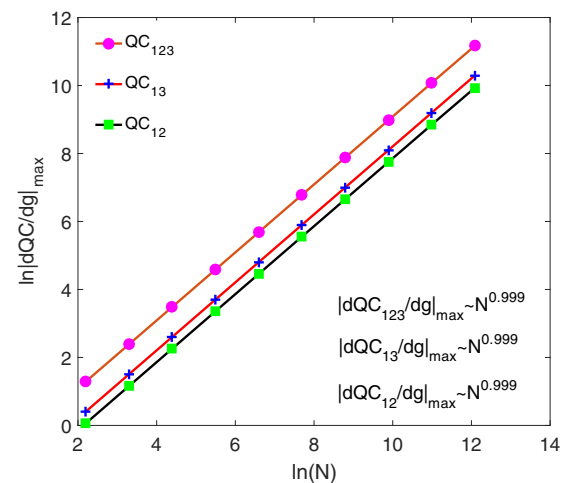


FIG. 4. Logarithm of the absolute value of the maximum $\ln|dQC_{123}/dg|_{\max}$, $\ln|dQC_{13}/dg|_{\max}$, and $\ln|dQC_{12}/dg|_{\max}$ vs the logarithm of the chain size $\ln(N)$.

this system $\rho = \sum_i \exp(-E_i)|\psi_i\rangle\langle\psi_i|$ is obtained. Under the Schrödinger picture, the evolution is described by unitary

operator $U(t) = e^{-iHt}$. If we choose $\rho_0 = \sum_i p_i|\psi_0\rangle\langle\psi_0|$ as the initial state, then the final state is

$$\rho_t = \sum_i p_i U(t)|\psi_0\rangle\langle\psi_0|U^\dagger(t) = U(t)\rho_0U^\dagger(t). \tag{18}$$

The expression $U(t)$ in this model is defined as

$$U(t) = \begin{pmatrix} \frac{\eta_1}{2k^2} & 0 & 0 & U_2(t) & 0 & U_6(t) & U_2(t) & 0 \\ 0 & U_{10}(t) & U_3(t) & 0 & U_8(t) & 0 & 0 & U_1(t) \\ 0 & U_3(t) & \frac{\eta_2}{2k^2} & 0 & U_3(t) & 0 & 0 & U_5(t) \\ U_2(t) & 0 & 0 & U_9(t) & 0 & U_4(t) & U_7(t) & 0 \\ 0 & U_8(t) & U_3(t) & 0 & U_{10}(t) & 0 & 0 & U_1(t) \\ U_6(t) & 0 & 0 & U_4(t) & 0 & \frac{\eta_3}{2k^2} & U_4(t) & 0 \\ U_2(t) & 0 & 0 & U_7(t) & 0 & U_4(t) & U_9(t) & 0 \\ 0 & U_1(t) & U_5(t) & 0 & U_1(t) & 0 & 0 & \frac{\eta_4}{2k^2} \end{pmatrix}, \tag{19}$$

where $\eta_1 = 2U_{12}(t) + \gamma^2(U_{14}(t) + U_{13}(t))$, $\eta_2 = 2U_{11}(t)\gamma^2 + U_{17}(t) + U_{16}(t)$, $\eta_3 = 2U_{12}(t) + U_{14}(t) + U_{13}(t)$, $\eta_4 = 2U_{11}(t) + \gamma^2(U_{17}(t) + U_{16}(t))$, $U_1(t) = \frac{\sqrt{2\gamma U_{17}(t)} - \sqrt{2\gamma U_{16}(t)}}{4k}$, $U_2(t) = \frac{\sqrt{2\gamma U_{14}(t)} - \sqrt{2\gamma U_{13}(t)}}{4k}$, $U_3(t) = \frac{\sqrt{2}U_{17}(t) - \sqrt{2}U_{16}(t)}{4k}$, $U_4(t) = \frac{\sqrt{2}U_{14}(t) - \sqrt{2}U_{13}(t)}{4k}$, $U_5(t) = \frac{-2\gamma U_{11}(t) + \gamma U_{17}(t) + \gamma U_{16}(t)}{2k^2}$, $U_6(t) = \frac{-2\gamma U_{12}(t) + \gamma U_{14}(t) + \gamma U_{13}(t)}{2k^2}$, $U_7(t) = -U_{15}(t) + \frac{U_{14}(t) + U_{13}(t)}{4}$, $U_8(t) = -U_{18}(t) + \frac{U_{17}(t) + U_{16}(t)}{4}$, $U_9(t) = U_{15}(t) + \frac{U_{14}(t) + U_{13}(t)}{4}$, $U_{10}(t) = U_{18}(t) + \frac{U_{17}(t) + U_{16}(t)}{4}$, $U_{11}(t) = e^{-d_4 t i}$, $U_{12}(t) = e^{-d_2 t i}$, $U_{13}(t) = e^{-d_7 t i}$, $U_{14}(t) = e^{-d_5 t i}$, $U_{15}(t) = e^{-d_3 t i} / 2$, $U_{16}(t) = e^{-d_8 t i}$, $U_{17}(t) = e^{-d_6 t i}$, $U_{18}(t) = e^{-d_1 t i} / 2$.

(1) We first take $\psi_0 = |000\rangle$ as the initial state; the density matrix reads

$$\rho_0 = \begin{pmatrix} 1 & 0 & 0 & 0 & 0 & 0 & 0 & 0 \\ 0 & 0 & 0 & 0 & 0 & 0 & 0 & 0 \\ 0 & 0 & 0 & 0 & 0 & 0 & 0 & 0 \\ 0 & 0 & 0 & 0 & 0 & 0 & 0 & 0 \\ 0 & 0 & 0 & 0 & 0 & 0 & 0 & 0 \\ 0 & 0 & 0 & 0 & 0 & 0 & 0 & 0 \\ 0 & 0 & 0 & 0 & 0 & 0 & 0 & 0 \\ 0 & 0 & 0 & 0 & 0 & 0 & 0 & 0 \end{pmatrix}. \tag{20}$$

Under the unitary time evolution operator, the density matrix of the system becomes

$$\rho_t = \begin{pmatrix} \xi_6^2 & 0 & 0 & \xi_1 & 0 & \xi_4 & \xi_1 & 0 \\ 0 & 0 & 0 & 0 & 0 & 0 & 0 & 0 \\ 0 & 0 & 0 & 0 & 0 & 0 & 0 & 0 \\ -\xi_1 & 0 & 0 & \xi_3 & 0 & -\xi_2 & \xi_3 & 0 \\ 0 & 0 & 0 & 0 & 0 & 0 & 0 & 0 \\ \xi_4 & 0 & 0 & \xi_2 & 0 & \zeta & \xi_2 & 0 \\ -\xi_1 & 0 & 0 & \xi_3 & 0 & -\xi_2 & \xi_3 & 0 \\ 0 & 0 & 0 & 0 & 0 & 0 & 0 & 0 \end{pmatrix}, \tag{21}$$

where $\xi_1 = \frac{\sqrt{2} \sin(\frac{\xi_5}{2})(g-1)^2 i}{2k(g+1)}$, $\xi_2 = \frac{\sqrt{2}(\sin(\xi_5) - 2 \sin(\frac{\xi_5}{2}))(g-1)^2 i}{4k^3(g+1)^2}$, $\xi_3 = \frac{\sin(\xi_5/2)^2(g-1)^2}{\xi_8}$, $\xi_4 = \frac{e^{-\xi_9/2} \xi_7^2 (g-1) \xi_6}{2k^2(g+1)}$, $\xi_5 = \sqrt{2}Jkt$, $\xi_6 = \frac{1}{k^2} + \frac{e^{-\xi_9/2}(g-1)^2}{\xi_8} + \frac{e^{\xi_9/2}(g-1)^2}{\xi_8}$, $\xi_7 = e^{\xi_9/2} - 1$, $\xi_8 = 2k^2(g+1)^2$, $\xi_9 = \sqrt{2}Jkti$, $\zeta = \frac{e^{-\xi_9} \xi_7^2 (g-1)^2}{4k^4(g+1)^2}$.

The analytic expression of the quantum coherence of Eq. (21) is

$$QC_{l_1}(\rho_t) = 4|\xi_1| + 4|\xi_2| + 2|\xi_3| + 2|\xi_4|. \tag{22}$$

Figure 5 displays the evolution of quantum coherence under different QRG steps. We notice that the quantum coherence oscillates over time. It is clear that the fluctuations have a period T that one can understand from Eq. (22). As iterations of QRG increase, the oscillation of the quantum coherence versus the time will enhance. The maximum value for each curve increases gradually, and finally will keep stable as the QRG steps become larger than 5. Figure 5 also shows that the period T decreases as the size of the system increases. Moreover, the conservation property of every quantum coherence still exists in this case.

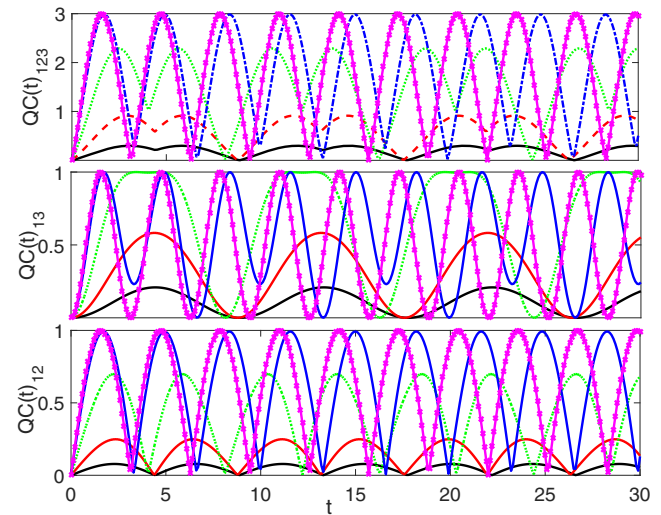


FIG. 5. Quantum coherence of the XY model as a function of t when $J=1$, $g=0.9$, and $\rho_0 = |000\rangle\langle 000|$. The black solid line means 0th QRG step, red dashed line means 1st QRG step, green dotted line means 2nd QRG step, blue dot-dashed line means 3rd QRG step, and purplish red cross markers mean 4th QRG step. All the parameters are dimensionless.

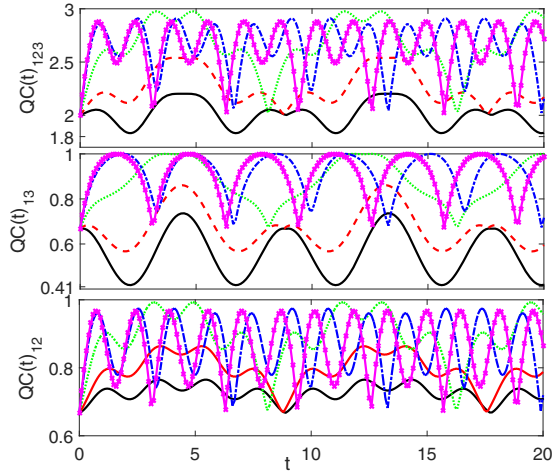


FIG. 6. Quantum coherence of the XY model as a function of t when $J=1$, $g=0.9$, and $\psi_0 = (|100\rangle + |010\rangle + |001\rangle)/\sqrt{3}$. The black solid line means 0th QRG step, red dashed line means 1st QRG step, green dotted line means 2nd QRG step, blue dot-dashed line means 3rd QRG step, and purple cross markers mean 4th QRG step. All the parameters are dimensionless.

(2) We next consider the three-qubit W state $\psi_0 = (|100\rangle + |010\rangle + |001\rangle)/\sqrt{3}$ as the initial state. The analytical results of quantum coherence are not given here for the tedious expressions. Figure 6 shows the numerical simulation results. We can see that the quantum coherence still demonstrates the periodic oscillation property with time. The performance of quantum coherence is not the same as the $\psi_0 = |000\rangle$ case. The difference is that the maximum value will be attained only after the 2nd QRG step. The periodic oscillations of $QC(t)_{123}$, $QC(t)_{13}$, and $QC(t)_{12}$ are identical for every QRG iteration steps. This property again proves that the reduced density matrix may represent the whole system.

VI. SUMMARY

To sum up, we have studied the low-energy-state dynamic of quantum coherence in the anisotropic XY spin system by using QRG theory. The critical property of the model is obtained through renormalization of the spin chain. We have derived the analytical expressions of quantum coherence for the block state and its reduced state. The divergent characteristic of the first derivative of quantum coherence was accompanied by the scaling behavior near the quantum phase transition point. We also find that the block state and the reduced state both display similar scaling properties with identical coherence exponents 0.999. This implies that we may get the composite system results by its reduced density matrix. Furthermore, by

considering the dynamical factor, we study the evolution of the XY model in low-energy states. The dynamical factor of the model could reveal the fingerprint of the quantum critical property for an infinite-size system. The analysis of quantum coherence in the XY systems may not only promote insight into its critical behavior but may also be applied to quantum information processing.

ACKNOWLEDGMENTS

This work was supported by the Natural Science Foundation of Jiangsu Province, China (Grant No. BK20171397), the Pre-research Foundation of Army Engineering University and the Foundation of Department of General Education, the National Natural Science Foundation of China (Grants No. 11535004, No. 11035001, No. 11165006, No. 10735010, and No. 10975072), the 973 National Major State Basic Research and Development of China (Grants No. 2013CB834400 and No. 2010CB327803), and the Project Funded by the Priority Academic Programme Development of Jiangsu Higher Education Institutions (PAPD).

APPENDIX

We have derived the renormalized equation $\gamma' = \frac{\gamma^3 + 3\gamma}{3\gamma^2 + 1}$. This equation can be solved by iteration, such as if we begin from γ_0 , and then get $\gamma_1 = \gamma'_0$, after that we get $\gamma_2 = \gamma'_1$ from γ_1 , etc. The sequence of $\{\gamma_0, \gamma_1, \gamma_2, \gamma_3, \dots, \gamma_n\}$ produces the flow of the renormalization group. This sequence represents a continuous manipulation of spin on an infinite chain and converts it into a new effective spin [26]. The scale of the system is rescaled with factor $b = 3$ in each operation. In this way, the coherence of the system also changed with different γ . For example, the coherence is

$$QC_{l_1}(\rho_{13}) = \frac{1}{2} + \frac{|\gamma|}{\gamma^2 + 1},$$

$$QC_{l_1}(\rho_{12}) = C_{l_1}(\rho_{23}) = \frac{\sqrt{2}}{2\sqrt{\gamma^2 + 1}} + \frac{\sqrt{2}|\gamma|}{2\sqrt{\gamma^2 + 1}}; \quad (\text{A1})$$

in 0th renormalization, the coherence is

$$QC_{l_1}(\rho_{13}) = \frac{1}{2} + \frac{|\gamma^3 + 3\gamma|(3\gamma^2 + 1)}{(\gamma^3 + 3\gamma)^2 + (3\gamma^2 + 1)^2},$$

$$QC_{l_1}(\rho_{12}) = C_{l_1}(\rho_{23}) = \frac{\sqrt{2}(3\gamma^2 + 1)}{2\sqrt{(\gamma^3 + 3\gamma)^2 + (3\gamma^2 + 1)^2}} \times \left(1 + \left|\frac{\gamma^3 + 3\gamma}{3\gamma^2 + 1}\right|\right) \quad (\text{A2})$$

in 1st renormalization, and so on.

- [1] H. D. Young, R. A. Freedman, and A. L. Ford, *Sears and Zemansky's University Physics with Modern Physics*, 12th ed. (Addison-Wesley, Boston, 2012).
- [2] M. A. Nielsen and I. L. Chuang, *Quantum Computation and Quantum Information* (Cambridge University Press, Cambridge, 2010).

- [3] J. J. Sakurai and J. Napolitano, *Modern Quantum Mechanics*, 2nd ed. (Addison-Wesley, Boston, 2010).
- [4] X. Yuan, H. Zhou, Z. Cao, and X. Ma, *Phys. Rev. A* **92**, 022124 (2015).
- [5] Y. T. Wang, J. S. Tang, Z. Y. Wei, S. Yu, Z. J. Ke, X. Y. Xu, C. F. Li, and G. C. Guo, *Phys. Rev. Lett.* **118**, 020403 (2017).

- [6] Z. He, L. Li, C. M. Yao, and Y. Li, *Acta Phys. Sin.* **64**, 140302 (2015).
- [7] T. Baumgratz, M. Cramer, and M. B. Plenio, *Phys. Rev. Lett.* **113**, 140401 (2014).
- [8] D. Girolami, *Phys. Rev. Lett.* **113**, 170401 (2014).
- [9] L. H. Shao, Z. J. Xi, H. Fan, and Y. M. Li, *Phys. Rev. A* **91**, 042120 (2015).
- [10] A. Streltsov, U. Singh, H. S. Dhar, M. N. Bera, and G. Adesso, *Phys. Rev. Lett.* **115**, 020403 (2015).
- [11] T. R. Bromley, M. Cianciaruso, and G. Adesso, *Phys. Rev. Lett.* **114**, 210401 (2015).
- [12] E. Chitambar, A. Streltsov, S. Rana, M. N. Bera, G. Adesso, and M. Lewenstein, *Phys. Rev. Lett.* **116**, 070402 (2016).
- [13] A. Winter and D. Yang, *Phys. Rev. Lett.* **116**, 120404 (2016).
- [14] C. Napoli, T. R. Bromley, M. Cianciaruso, M. Piani, N. Johnston, and G. Adesso, *Phys. Rev. Lett.* **116**, 150502 (2016).
- [15] E. Chitambar and M. H. Hsieh, *Phys. Rev. Lett.* **117**, 020402 (2016).
- [16] J. J. Chen, J. Cui, Y. R. Zhang, and H. Fan, *Phys. Rev. A* **94**, 022112 (2016).
- [17] Y. Yao, X. Xiao, L. Ge, and C. P. Sun, *Phys. Rev. A* **92**, 022112 (2015).
- [18] J. J. Ma, B. Yadin, D. Girolami, V. Vedral, and M. Gu, *Phys. Rev. Lett.* **116**, 160407 (2016).
- [19] G. Karpat, B. Çakmak, and F. F. Fanchini, *Phys. Rev. B* **90**, 104431 (2014).
- [20] F. W. Ma, S. X. Liu, and X. M. Kong, *Phys. Rev. A* **83**, 062309 (2011).
- [21] Y. L. Xu, X. M. Kong, Z. Q. Liu, and C. C. Yin, *Phys. Rev. A* **95**, 042327 (2017).
- [22] M. Kargarian, R. Jafari, and A. Langari, *Phys. Rev. A* **76**, 060304 (2007).
- [23] M. Kargarian, R. Jafari, and A. Langari, *Phys. Rev. A* **77**, 032346 (2008).
- [24] R. Jafari, M. Kargarian, A. Langari, and M. Siahatgar, *Phys. Rev. B* **78**, 214414 (2008).
- [25] M. Qin, Z. Z. Ren, and X. Zhang, *Sci. Rep.* **6**, 26042 (2016).
- [26] G. J. Jin and D. Feng, *Prog. Phys.* **29**, 325 (2009) (in Chinese).